Electron-capture decay of ^{98}Tc

Dominik Elchine [1] Martin Müller [2] Markus Schiffer [2] and Erik Strub [1,*]

[1] Division of Nuclear Chemistry, University of Cologne, Zülpicher Str. 45, 50674 Cologne, Germany

[2] Institute for Nuclear Physics, University of Cologne, Zülpicher Str. 77, 50937 Cologne, Germany

(Received 17 April 2025; revised 16 July 2025; accepted 15 September 2025; published 22 October 2025)

From simple symmetry and energy considerations it can be concluded that ^{98}Tc might undergo electron capture decay (EC). In this work we provide evidence for an EC decay of ^{98}Tc measuring 2.67 g K[TcO_4] that contains approximately 1 GBq of ^{99}Tc. By use of a lead shielding for the sample, it was possible to identify the coincident $4+ \rightarrow 2+$ and $2+ \rightarrow 0 + \gamma$ transitions in the daughter nuclide ^{98}Mo at the University of Cologne's Cologne Clover Counting setup of the Institute for Nuclear Physics. For the first time, the EC/β^- branching ratio of 0.29(3)% was determined directly. With a log ft of 14.21(7) this decay does almost tie with the log ft of the ^{36}Cl EC decay [14.23(1)] for the same highest second forbidden nonunique transition.

DOI: 10.1103/y5d7-85w5

I. INTRODUCTION

It is well known that a fraction of the predominantly β^- emitting isotope ^{100}Tc undergoes electron capture (EC) decay [1]. It is to be expected that the lighter isotope ^{98}Tc might undergo EC or β^+ decay as well. The nuclear properties of ^{98}Tc and its potential EC daughter ^{98}Mo supports this hypothesis [2]: The Q value for the EC of ^{98}Tc into ^{98}Mo [$Q = 1684(3)$] is only slightly smaller than the Q value for the β^- decay into ^{98}Ru [$Q = 1793(7)$] [3]. Moreover, both daughter nuclei exhibit very similar level schemes. The ^{98}Tc ground state has a nuclear spin of 6+, and both EC and β^- can feed a 4+ nuclear state in the respective daughter nucleus. Also, in both daughter nuclei, this 4+ state can be deexcited in a two-step cascade via a 2+ state into the 0+ ground state (Fig. 1). While the β^- decay is followed by coincident γ-ray lines at 745.4 keV and 652.5 keV, EC should be followed by coincident γ-ray lines at 722.6 keV and 787.4 keV, respectively. The associated change in angular momentum of $\Delta J = 2$ without a change of parity, $\Delta\pi =$ no, is classified as second forbidden non-unique transition, with a lower limit for the log ft value of 11.0 [5], similar to the β^- transition of ^{98}Tc with log $ft = 13.984(48)$ [5]. Energetically, a β^+ decay of ^{98}Tc into the ground state of ^{98}Mo would be possible, but is strongly forbidden due to the large difference of angular momentum $\Delta J = 6$.

A. Previous results

Earlier research on this subject by Kobayashi could not identify the expected transitions at 722.6 keV and 787.4 keV. Kobayashi estimated an upper limit for the EC branching ratio of $< 4\%$ [4]. The measurements were performed using an ^{99}Tc sample containing traces of ^{98}Tc, providing a relatively easy access, as ^{99}Tc can be obtained in quantities of a few grams. It is a fission product with a cumulative fission yield (FY) of 6.139% (from fission of ^{235}U) or 6.14% (from fission of ^{239}Pu) and it always contains traces of ^{98}Tc [6]. While the decay chain of most fission products with $A = 98$ end up in stable ^{98}Mo, there is always a small contribution of ^{98}Tc from direct fission [$5.4(18) \times 10^{-9}$% from fission of ^{235}U and $4.6(18) \times 10^{-7}$% from fission of ^{239}Pu] [7,8]. In a sample of 1 g, this amounts to 3×10^{13} to 3×10^{15} atoms of ^{98}Tc or roughly 0.4 to 40 Bq. 2.67 g K[$^{99}TcO_4$] is equivalent to 1.31 g of ^{99}Tc. This γ activity can be detected with germanium detectors despite the large surplus of ^{99}Tc activity by the 745.4 keV and 652.5 keV lines, if the beta particles of ^{99}Tc are shielded adequately. Besides these beta particles, ^{99}Tc emits only a weak ($I = 0.00065\%$) low energy 89.5 keV gamma-ray line [9]. Therefore, the lines of ^{98}Tc at 722.6 keV and 787.4 keV are detectable, providing sufficient measurement time.

B. Experimental setup

A sample of 2.67 g K[$^{99}TcO_4$] [Fig. 2(a)] was measured at the University of Cologne's Cologne Clover Counting setup of the Institute for Nuclear Physics, a pair of detectors each consisting of four coaxial N-type HPGe crystals [10]. The sample was enclosed in a cylindrical lead container with 0.58 cm thick walls [Fig. 2(b)] to suppress β radiation, Bremsstrahlung, and most of the 89.5 keV γ-ray line as well as any x-ray fluorescence originating from the β^- decay. The sample was measured for 407 h. The absorption of the 722.6 keV and 787.4 keV γ-ray lines in the lead shielding is taken into account by a relative efficiency calibration, which is affected by absorption in the same way.

II. RESULTS

The measured γ spectrum (Fig. 3) shows both the known signature of the β^- decay at 745.4 keV and 652.5 keV and the γ-ray lines at 722.6 keV and 787.4 keV indicating EC.

*Contact author: erik.strub@uni-koeln.de

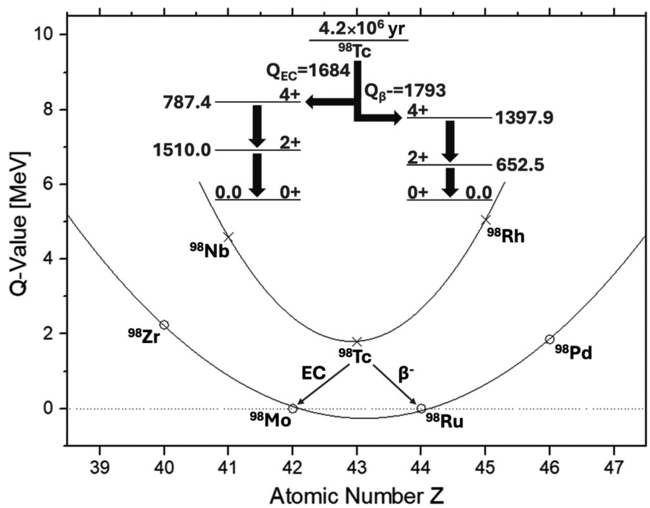

FIG. 1. Isobaric lines for mass number $A = 98$ in the range of atomic number $Z = 39$ to 47 [2].

The almost complete absence of the γ-ray line at 89.5 keV confirms the sufficient lead shielding. The signal at 661.7 keV is attributed to the ^{137}Cs β^- decay, which is present in the sample as a contaminant [11]. ^{99}Tc samples typically contain ^{137}Cs, as it is one of the main fission products with a specific activity roughly 5 orders of magnitude higher than that of ^{98}Tc. It is essential to keep the ^{137}Cs content low in order to quantitively evaluate the ^{98}Tc 652.5 keV line. In the spectrum, an activity of about 1 Bq associated with the ^{98}Tc EC decay could be directly detected despite a background activity of about 1 GBq of ^{99}Tc. Even this small activity is higher than estimated from the FY (given above).

In Tables I and II, the data from the peak evaluation are given. All peaks were fitted with origin as Gauss peaks with additional low-energy-tailing. The spectra of the clover detector B0 were not used for the evaluation due to a lower energy resolution of this detector. In this detector, the lower resolution prevents clear identification and removal of a contamination at 725 keV (most probably originating from the ^{232}Th decay series) from the gamma line at 722.6 keV.

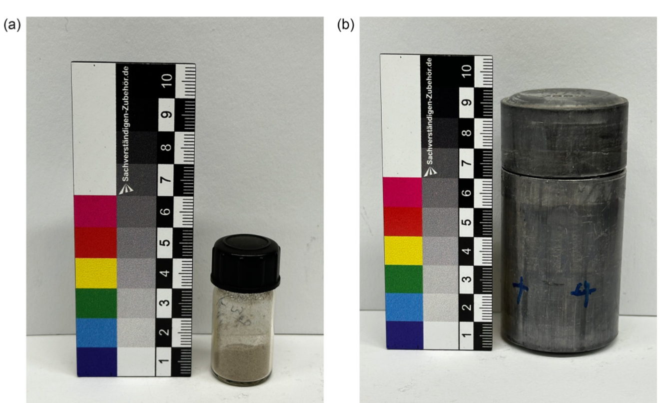

FIG. 2. (a) Sample of 2.67 g of K[^{99}TcO$_4$]. (b) Cylindrical lead enclosure measuring 8.58 cm in height, 4.24 cm in outer diameter and 0.58 cm in wall thickness. The provided scale is in “cm”.

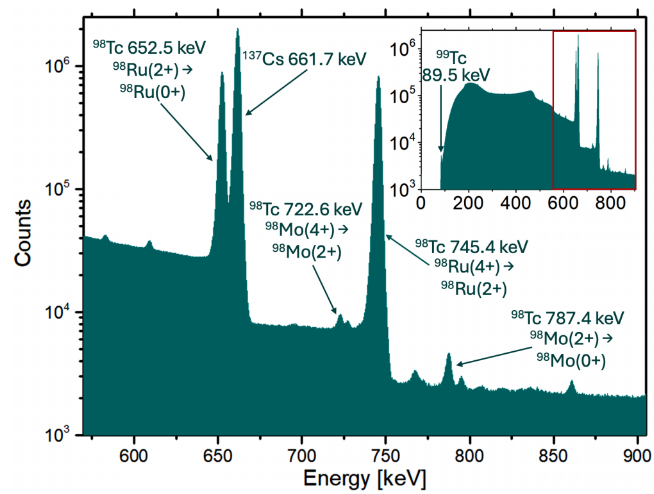

FIG. 3. Section of the measured γ spectrum showing both transitions $4+ \rightarrow 2+$ and $2+ \rightarrow 0+$ in the daughter nuclides of the β^- decay (^{98}Ru) and EC (^{98}Mo). The spectrum shown here is the sum of the spectra of all eight clover detectors. The single spectra were separately energy-calibrated before summing.

Further information is provided by correlation data from the two-step cascade (Fig. 4). In this process, the single energy is plotted against the sum energy of coincident events.

The correlation between the individual photopeaks from the $4+ \rightarrow 2+$ (722.6 keV) and $2+ \rightarrow 0+$ (787.4 keV) transitions and the sum peak at 1510 keV are clearly visible. This indicates that the two signals are detected in coincidence, confirming the EC decay for the ^{98}Tc. The prominent vertical line at 1397.9 keV represents the sum energy of both transitions after the β^- decay. It correlates with both individual transitions $4+ \rightarrow 2+$ (745.4 keV) and $2+ \rightarrow 0+$ (652.5 keV).

For the calculation of the branching ratio, corresponding to the EC decay, an internal efficiency calibration was performed, comparing both ^{98}Ru lines, each with 100% intensity. As all lines of interest fall within a narrow energy range, internal efficiency calibration was considered more precise than an efficiency calibration with reference samples, however, an additional efficiency calibration using calibration standards was performed as well. Both calibration methods are in very good agreement.

For the internal efficiency calibration, the efficiency at 652.5 keV was set to 100%. Then, the relative efficiency at 745.4 keV was calculated comparing the intensities of the 745.4 keV and 652.5 keV lines. The efficiency at the 722.6 keV transition was calculated by linear interpolation between the energies of the two ^{98}Ru lines using

$$\varepsilon_{722.6\,\mathrm{keV}} = 100\% + \Delta E_1 \times \frac{\Delta\varepsilon}{\Delta E_2} \tag{1}$$

with $\Delta E_1 = (722.6\text{–}652.5)\,\mathrm{keV}$, $\Delta E_2 = (745.4\text{–}652.5)\,\mathrm{keV}$, and $\Delta\varepsilon = \varepsilon_{745.4\,\mathrm{KeV}} - \varepsilon_{652.5\,\mathrm{KeV}}$.

Finally, the efficiency at the 787.4 keV transition was determined using extrapolation accordingly.

The resulting efficiencies are given in Table III.

TABLE I. γ signal counts from β^- decay into ^{98}Ru, background, and associated 1-σ count rate uncertainties. Uncertainties are derived from the statistical uncertainty of signal and background counts.

Detector name	Counts at 745.4 keV	Background 745.4 keV	Count rate error [%]	Counts at 652.5 keV	Background 652.5 keV	Count rate error [%]
A0	1961887	117793	0.074	2014057	659455	0.081
A1	1969092	107135	0.073	2077566	556485	0.078
A2	1599692	92679	0.081	1655383	547202	0.090
A3	2078091	108425	0.071	2182232	626442	0.077
B1	2488933	127384	0.065	2702213	717374	0.068
B2	1942531	102374	0.074	2148319	509113	0.076
B3	2254718	118118	0.068	2418498	694685	0.073

TABLE II. γ signal counts from EC decay into ^{98}Mo, background, and associated 1-σ count rate uncertainties. Uncertainties are derived from the statistical uncertainty of signal and background counts.

Detector name	Counts at 722.6 keV	Background 722.6 keV	Count rate error [%]	Counts at 787.4 keV	Background 787.4 keV	Count rate error [%]
A0	6231	81730	4.760	6893	25787	2.622
A1	5314	99668	6.097	6127	27386	2.988
A2	4456	89473	6.878	4855	26317	3.637
A3	6080	74619	4.673	6352	22324	2.666
B1	6446	87528	4.756	6342	31588	3.071
B2	5317	73312	5.274	5549	27036	3.253
B3	6410	79309	4.568	6418	32473	3.073

TABLE III. Internal efficiency calibration. 1-σ uncertainties given in parentheses. Uncertainties of the efficiencies are derived by uncertainty propagation from the statistical uncertainty of the signals following the β^- decay into ^{98}Ru (see Table I).

Detector name	Rel. efficiency at 652.5 keV [%]	Rel. efficiency at 745.4 keV [%]	Rel. efficiency at 722.6 keV [%]	Rel. efficiency at 787.4 keV [%]
A0	100	97.4(1)	98.0(1)	96.2(1)
A1	100	94.8(1)	96.1(1)	92.5(1)
A2	100	96.6(1)	97.4(1)	95.1(1)
A3	100	95.2(1)	96.4(1)	93.0(1)
B1	100	92.1(1)	94.0(1)	88.6(1)
B2	100	90.4(1)	93.0(1)	86.3(1)
B3	100	93.2(1)	94.9(1)	90.2(1)

TABLE IV. EC/β^- branching ratios derived from ^{98}Mo γ lines at 722.6 keV and 787.4 keV. 1-σ uncertainties given in parentheses. Uncertainties are derived by uncertainty propagation from the efficiency calibration (see Table III), the signal counts from β^- decay into ^{98}Ru (see Table I) and the signal counts from EC decay into ^{98}Mo (see Table II).

Detector name	Branching from 722.6 keV [%]	Propagated error for 722.6 keV [%]	Branching from 787.4 keV [%]	Propagated error for 787.4 keV [%]
A0	0.32(2)	4.76	0.36 (1)	2.62
A1	0.27(2)	6.10	0.32(1)	3.00
A2	0.28(2)	6.88	0.31(1)	3.64
A3	0.29(1)	4.67	0.31(1)	2.67
B1	0.25(1)	4.76	0.27(1)	3.07
B2	0.27(1)	5.28	0.30(1)	3.26
B3	0.28(1)	4.57	0.29(1)	3.07

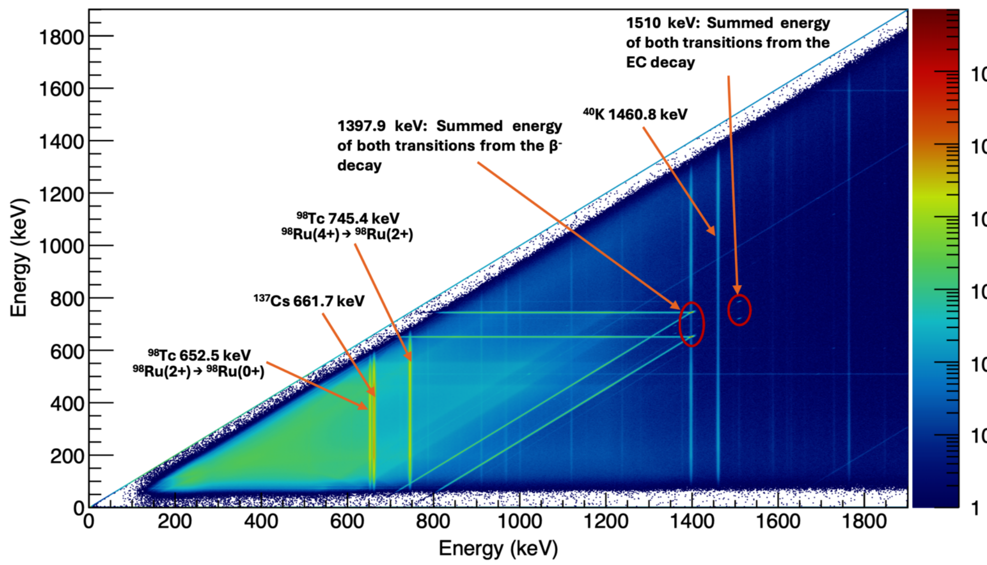

FIG. 4. Two-step cascade (TSC) matrix [12]. The TSC matrix contains all events in which any two leaves of the detector setup detected a signal within a coincidence window of 60 ns. On the x-axis the total energy of the event is shown, while the y axis corresponds to the energy detected by each individual leaf (i.e., two entries per event). The color encodes the number of entries per 1 keV × 1 keV bin. [2,11,13].

Applying these efficiencies, the EC/β^- branching ratio can be independently determined from the two lines at 722.6 keV and 787.4 keV (Table IV and Figs. 5 and 6).

The calculated branching ratio of the EC/β^- for the 722.6 keV line, is 0.28(3)%, and 0.31(3)% for the corresponding line at 787.4 keV. This results in an overall branching ratio of the EC/β^- of 0.29(3)%, which is also consistent with the upper limit estimate of < 4% by Kobayashi [4].

The log ft value was determined using two components: the t value derived from the half-life of $4.2(3) \times 10^6$ y and the experimentally measured branching ratio of 0.29(3). The f-value was calculated using the latest released version (v2.4) of the BetaShape code [7]. This determines a logft of 14.21(7), which is consistent with a second forbidden nonunique transition.

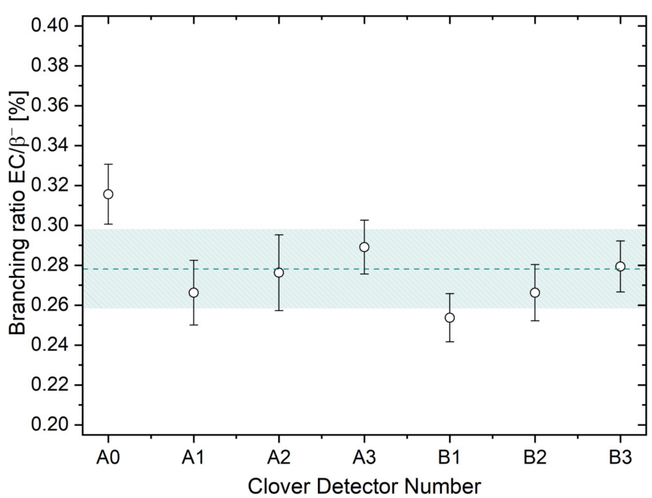

FIG. 5. Branching ratio of EC/β^- decay for all Clover segments, calculated from the 722.6 keV line, are represented by circular symbols with vertical error bars. The error bars reflect the statistical uncertainties of the single values as given in Table IV. The dashed line and the shaded region indicate the arithmetic mean and deviation from the arithmetic mean. All reported uncertainties are given at the 1-σ confidence level.

III. DISCUSSION

For the first time, the suspected EC decay of ^{98}Tc was observed, enabling the determination of a branching ratio for the EC/β^- decay, found to be 0.29% ± 0.03% (1-σ confidence level). The measurement became possible due to proper sample shielding (Fig. 7). With this it is not only possible to identify several Bq of ^{98}Tc in a 1 GBq ^{99}Tc sample, but also to quantify the EC which is 2 orders of magnitude lower, corresponding to an activity ratio of $<10^{-9}$. The observed activity of ^{98}Tc is higher than expected from the tabulated direct FYs.

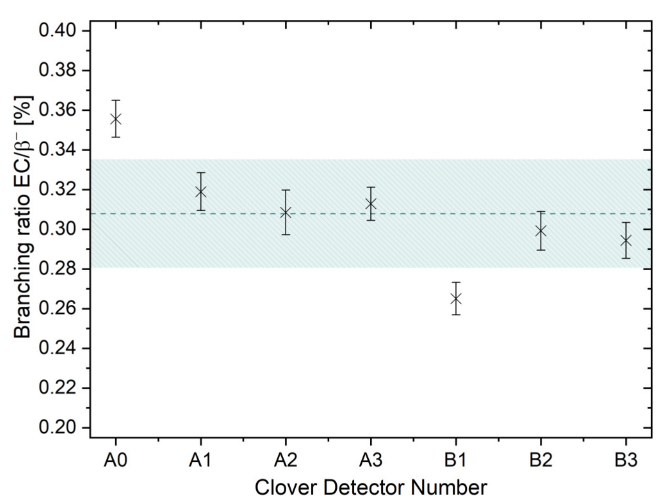

FIG. 6. Same as Fig. 5 but for the 787.4 keV line.

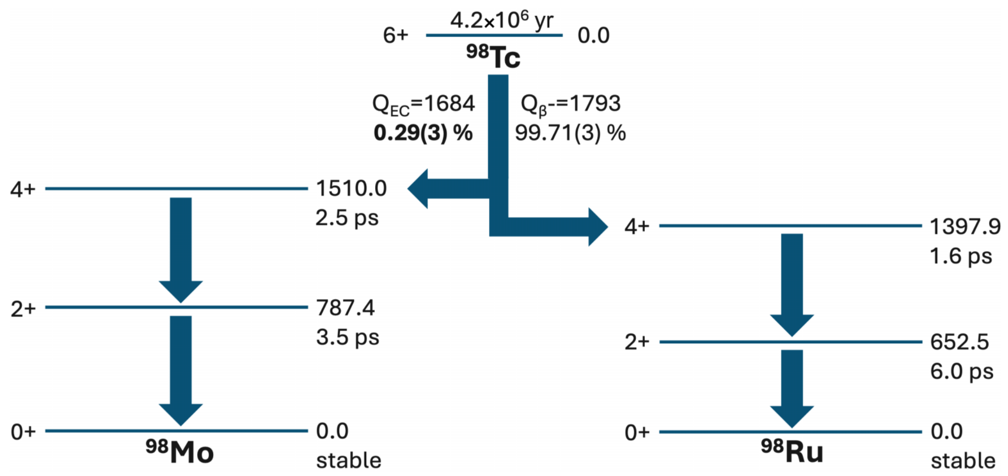

FIG. 7. Decay scheme of ^{98}Tc [2], with newly measured decay branching ratios from the current work.

Currently, the direct FYs are given in the literature with relative uncertainties in the range of 30% to 40%. In principle, it could be attempted to redetermine the FYs of ^{98}Tc based on precise decay data, however this is practically not possible without detailed knowledge on the reactor in which the ^{98}Tc was produced: first, the FY depends strongly on the exact fuel composition; the ^{239}Pu FY is 2 orders of magnitude higher than the ^{235}U FY. Second, ^{98}Tc will also be produced by the ^{99}Tc $(n,\ 2n)$ ^{98}Tc reaction with fast neutrons, thus depending on the neutron spectrum of the reactor. In fact, the ^{98}Tc/^{99}Tc ratio in the used sample is higher than estimated from FYs, giving evidence that the $(n,2n)$ reaction was the dominant production path in the given sample.

With a $\log ft$ of 14.21(7), corresponding to a partial half-life of $>10^9$ y, this decay does almost tie with the $\log ft$ of the ^{36}Cl decay [14.23(1)], which has the highest known logft value for a second forbidden non-unique transition, $\Delta J = 2$ and $\Delta\pi =$ no.

Systematically, studying EC decays with similar logft values could provide valuable information for testing nuclear models.

The new decay path might have implications for ^{98}Tc produced in meteorites, but also to ^{98}Tc found in terrestrial archives, where it can serve as a cosmochronometer [14] and in investigations of neutrino-induced reactions [15].

ACKNOWLEDGMENTS

This project has been supported by the Deutsche Forschungsgemeinschaft under Contract No. ZI 510/12–1.

DATA AVAILABILITY

The data that support the findings of this article are not publicly available. The data are available from the authors upon reasonable request.

[1] B. Singh and J. Chen, Nucl. Data Sheets **172**, 1 (2021).
[2] J. Chen and B. Singh, Nucl. Data Sheets **164**, 1 (2020).
[3] M. Wang, W. J. Huang, F. G. Kondev, G. Audi, and S. Naimi, Chin. Phys. C **45**, 030003 (2021).
[5] S. Turkat, At. Data Nucl. Data Tables **152**, 101584 (2023).
[4] T. Kobayashi, K. Sueki, M. Ebihara, H. Nakahara, M. Imamura, and A. Masuda, Radiochim. Acta **63**, 29 (1993).
[6] NEA, *The JEFF-3.1.1 Nuclear Data Library* (OECD Publishing, Paris, 2009).
[7] BetaShape code v.2.4 (11/6/2024), http://www.lnhb.fr/home/rd-activities/spectrum-processing-software/.
[8] R. W. Mills, EPJ Web Conf. **146**, 04008 (2017).
[9] E. Browne and J. K. Tuli, Nucl. Data Sheets **145**, 25 (2017).
[10] M. Müller, F. Heim, Y. Wang, S. Wilden, and A. Zilges, Phys. Rev. C **107**, 035804 (2023).
[11] E. Browne and J. K. Tuli, Nucl. Data Sheets **108**, 2173 (2007).
[12] A. M. Hoogenboom, Nucl. Instrum. **3**, 57 (1958).
[13] J. Chen, Nucl. Data Sheets **140**, 1 (2017).
[14] H. Becker, Chem. Geol. **196**, 43 (2003).
[15] T. Hayakawa *et al.*, Phys. Rev. Lett. **121**, 102701 (2018).